Anal. Chem. **2000,** *72,* 777−790

Tuning of an Electrospray Ionization Source for Maximum Peptide-Ion Transmission into a Mass Spectrometer

Scott Geromanos,[†] Gordon Freckleton,[†] and Paul Tempst*[,†,‡]

Protein Center and Molecular Biology Program, Memorial Sloan-Kettering Cancer Center, 1275 York Avenue, New York, New York 10021

We describe assembly and optimization of a continuous flow nanoelectrospray source for high-performance analysis on a routine basis. It is derived from an in*J*ection *a*daptable *F*ine *I*onization *S*ource ("JaFIS"), previously shown to be durable and easy to use (Geromanos, S.; et al. *Rapid Commun. Mass Spectrom.* 1998, *12*, 551−556) and now modified for maximum sensitivity. Proper design, manufacturing, and quality control of spray needles with specific orifice diameters, in combination with precisely controlled helium backpressure and applied voltage, enable stable flows at 1−2 nL/min. Needle positioning and ion spray potential are hereby exceedingly important, as shifts by 0.5 mm or 25 V, respectively, cause significant reduction in signal strength. In addition to prolonged analysis times, ultralow flows also yield higher sensitivity, the result of an improved "overall ion transfer efficiency" measured to be ∼5% at 1.6 nL/min. Used in combination with a "microtip" (Erdjument-Bromage, H.; et al. *J. Chromatogr. A* 1998, *826*, 167−181), the optimized JaFIS implements infusion-style ESI-MS at sensitivities approaching capillary LC-MS. Spraying times in excess of 20 h allow for any number of tandem mass spectrometric analysis routines to be performed, and to average thousands of scans in every experiment, thereby further improving sensitivity. This was fully illustrated by extensive analysis of a 2-fmol peptide mixture, in a 2-μL volume, using a multimode MS approach.

Completion of the genome project will lead to an even bigger challenge, interpreting the fluxes and flows of material and signals that result in cell behavior. The analysis of gene products, proteins, will likely take central position in this endeavor, as they drive life's vital processes.[1] Such include, among many, the control of when and where genes are expressed and the synthesis of most other molecules, big and small, in the cell. Gene expression is most readily monitored at the mRNA level,[2−4] except that such approaches may not provide an entirely accurate picture of the actual protein patterns.[5,6] A similar need exists to assess the physiologically active forms (i.e. processing and dynamic modifications) and the spatial/temporal interactions of proteins. Either way, protein identification laboratories should get ready to analyze larger numbers of samples, at increasingly higher levels of sensitivity and with turnaround times that allow orderly progression of the primary research projects. A mass spectrometric (MS) approach satisfies all three criteria, at least conceptually.[7−10]

In its elementary embodiment, "mass fingerprinting", a small set of proteolytic fragment masses—five or six but accurate to within 30−50 ppm—is sufficient to establish identity,[11−15] an experiment most easily done by matrix-assisted desorption/ionization (MALDI) reflectron time-of-flight (reTOF) MS.[14−17] Such a data set does not, however, allow one to query an expressed sequence tag (EST) database, nor is it usually enough to cope with mixed or contaminated proteins. In such instances, a multimode MS approach, particularly including electrospray ionization (ESI) tandem MS, is preferred.[16,18] Tandem MS enables protein identification on the basis of fragmentation data from a single, derivative peptide.[19−21] All commercially available tandem

* Corresponding author. E-mail: p-tempst@mskcc.org.
† Protein Center.
‡ Molecular Biology Program.

(1) Alberts, B. *Cell* **1998**, *92*, 291−294.
(2) Zhang, L.; Zhou, W.; Velculescu, V. E.; Kern, S. E.; Hruban, R. H.; Hamilton, S. R.; Vogelstein, B.; Kinzler, K. W. *Science* **1997**, *276*, 1268−1272.
(3) DeRisi, J. L.; Iyer, V. R.; Brown, P. O. *Science* **1997**, *278*, 680−686.
(4) Gerhold, D.; Rushmore, T.; Caskey, C. T. *Trends Biochem. Sci.* **1999**, *24*, 168−173.
(5) Gygi, S. P.; Rochon, Y.; Franza, B. R.; Aebersold, R. *Mol. Cell. Biol.* **1999**, *19*, 1720−1730.
(6) Oda, Y.; Huang, K.; Cross, F. R.; Cowburn, D.; Chait B. T. *Proc. Natl. Acad. Sci. U.S.A.* **1999**, *96*, 6591−6596.
(7) Mann, M. *Trends Biochem. Sci.* **1996**, *21*, 494−495.
(8) Roepsdorff, P. *Curr. Biol.* **1997**, *8*, 6−13.
(9) Yates III, J. R. *J. Mass Spectrom.* **1998**, *33*, 1−19.
(10) Haynes, P. A.; Gygi, S. P.; Figeys, D.; Aebersold, R. *Electrophoresis* **1998**, *19*, 1862−1871.
(11) Henzel, W. J.; Billeci, T. M.; Stults, J. T.; Wong, S. C.; Grimley, C.; Watanabe, C. *Proc. Natl. Acad. Sci. U.S.A.* **1993**, *90*, 5011−5015.
(12) Mann, M.; Højrup, P.; Roepstorff, P. *Biol. Mass Spectrom.* **1993**, *22*, 338−345.
(13) Pappin, D. J. C.; Højrup, P.; Bleasby, A. J. *Curr. Biol.* **1993**, *3*, 327−332.
(14) Jensen, O. N.; Podtelejnikov, A.; Mann, M. *Rapid Commun. Mass Spectrom.* **1996**, *10*, 1371−1378.
(15) Clauser, K. R.; Baker, P.; Burlingame, A. L. *Anal. Chem.* **1999**, *71*, 2871−2882.
(16) Shevchenko, A.; Jensen, O. N.; Podtelejnikov, A. V.; Sagliocco, F.; Wilm, M.; Vorm, O.; Mortensen, P.; Shevchenko, A.; Boucherie, H.; Mann, M. *Proc. Natl. Acad. Sci. U.S.A.* **1996**, *93*, 14440−14445.
(17) Ono, M.; Bolland, S.; Tempst, P.; Ravetch, J. V. *Nature* **1996**, *383*, 263−266.
(18) Neubauer, G.; King, A., Rappsilber, J.; Calvio, C.; Watson, M.; Ajuh, P.; Sleeman, J.; Lamond, A.; Mann, M. *Nat. Genet.* **1998**, *20*, 46−50.
(19) Eng, J. K.; McCormack, A. L.; Yates, J. R., III. *J. Am. Soc. Mass Spectrom.* **1994**, *5*, 976−989.
(20) Mann, M.; Wilm, M. *Anal. Chem.* **1994**, *66*, 4390−4399.

10.1021/ac991071n CCC: $19.00
Published on Web 01/08/2000

mass spectrometers utilize ESI, which involves the introduction of a sample in liquid form.

There are multiple ways to present an analyte solution to an ESI-MS instrument: direct infusion, liquid chromatogrpahic (LC), and capillary zone electrophoretic (CZE) systems, as well as the recently reported micromachined devices, which can be used in either configuration.[22−45] Both CZE- and LC-MS have the advantages of preionization concentration and adaptability to automation, but there are also drawbacks: higher flow rates, minimal MS/MS analysis time, more elaborate setup, and greater expertise required. Since CZE- and LC-MS are separation technologies, it is impossible to present the complete peptide mixture to the mass analyzer at any time. Although a mass spectrometer offers probably the best available separation technology, some of its value is lost when coupled to a CZE or LC. The single major disadvantage is the narrow window (typically less than 1 min) in which to conduct analysis. During this time, the operator has to determine the m/z, the charge state, and perform MS/MS. It provides for little, if any, user interaction in optimizing the fragmentation conditions, thus often resulting in lower quality data. The problem is compounded in case of coeluting peaks, having to perform two or three analyses in less than 1 min. When MS/MS data are of insufficient quality, ion series are difficult to ascertain and the user must rely solely (and blindly) on statistical analysis of uninterpreted spectra compared against a database. Although adequate algorithms have been written to assist in this type of identification,[19,46] large data sets must be generated for reliable results, especially in the case of "mixed" proteins.

In practice, partially fractionated complexes may be more suitably analyzed in a rational, interactive way by successive rounds of identification, until each protein has been positively confirmed. In this scheme, typically initiated with MALDI-TOF MS,[16] it is imperative that any peptide of the mixture can be selected at any time for MS/MS analysis, to either confirm a tentative identification or to analyze "orphan" precursor ions that do not yet map to an already identified protein, a process that may require a fair amount of time. The feasibility of the approach thus depends on continuous infusion of analytes at exceedingly low flows, a technique known as nanoelectrospray (nanoES).[31,32] In the absence of on-line LC, the sample concentration is most easily raised using off-line, micropreparative chromatographic devices ("microtips").[47,48] As a result, the microtip/nanoES method has evolved into an attractive, practical choice for peptide mixture mass analysis, a fact amply supported by numerous reports on protein identification in the context of authentic research problems.[49−54]

General emulation of this technique calls for a device that satifies the three major critera of routine use, simplicity, durability, and fault tolerance, yet offers uncompromized sensitivity and prolonged analysis times. Previously, we described an in*J*ection *a*daptable *F*ine *I*onization *S*ource ("JaFIS") that incorporated those desired practical features.[36] This report concerns maximum performance, more specifically sensitivity, which basically comes down to establishing conditions whereby the highest percentage of peptides will enter the mass spectrometer, and hit the detector, per unit time. A systematic examination, and subsequent optimization, of several key experimental variables was therefore conducted. To some extent, those efforts were guided by accepted theory about the electrospray process.[26,31,55−70]

(21) Fenyo, D.; Zhang, W., Chait, B. T.; Beavis, R. C. *Anal. Chem.* **1996**, *68*, 721A−726A.
(22) DeWit, J. S.; Parker, C. E.; Tomer, K. B.; Jorgenson, J. W. *Anal. Chem.* **1987**, *59*, 2400−2404.
(23) Emmett, M. R.; Caprioli, R. M. *J. Am. Soc. Mass Spectrom.* **1994**, *5*, 605−613
(24) Davis, M. T.; Stahl, D. C.; Hefta, S. A.; Lee, T. D. *Anal. Chem.* **1995**, *67*, 4549−4556.
(25) Davis, M. T.; Lee, T. D.. *J. Am. Soc. Mass Spectrom.* **1998**, *3*, 194−201.
(26) Ikonomou, M. G.; Blades, M. G.; Kebarle, P. *Anal. Chem.* **1990**, *14*, 1579−1583.
(27) Wahl, J. H.; Goodlett, D. R.; Udseth, H. R.; Smith, R. D. *Anal. Chem.* **1992**, *64*, 3194−3196.
(28) Figeys, D.; Ducret, A.; van Oostveen, I.; Aebersold, R. *Anal. Chem.* **1996**, *68*, 1822−1828.
(29) Figeys, D.; Ducret, A.; Yates, J. R., III; Aebersold, R. *Nat. Biotechnol.* **1996**, *14*, 1579−1583.
(30) Anden, P. E.; Emmett, M. R.; Caprioli, R. M *J. Am. Soc. Mass Spectrom.* **1994**, *5*, 867−869.
(31) Wilm, M. S.; Mann, M. *Int. J. Mass Spectrom. Ion Processes* **1994**, *136*, 167−180.
(32) Wilm, M. S.; Mann. M. *Anal. Chem.* **1996**, *68*, 1−8.
(33) Valaskovic, G. A.; Kelleher, N. L.; Little, D. P.; Aaserud, D. J.; McLafferty, F. W. *Anal. Chem.* **1995**, *67*, 3802−3805.
(34) Valaskovic, G. A.; McLafferty, F. W *J. Am. Soc. Mass Spectrom.* **1996**, *7*, 1270−1272.
(35) Hannis, J. C.; Muddiman, D. C. *Rapid Commun. Mass Spectrom.* **1998**, *12*, 443−448.
(36) Geromanos, S.; Philip, J.; Freckleton, G.; Tempst, P. *Rapid Commun. Mass Spectrom.* **1998**, *12*, 551−556.
(37) Ramsey, R. S.; Ramsey, J. M. *Anal. Chem.* **1997**, *69*, 1174−1178.
(38) Figeys, D.; Ning, Y.; Aebersold, R. *Anal. Chem.* **1997**, *69*, 3153−3160.
(39) Xue, Q.; Dunayevskiy, Y. M.; Foret, F.; Karger, B. L. *Rapid Commun. Mass Spectrom.* **1997**, *11*, 1253−1256.
(40) Xue, Q.; Foret, F.; Dunayevskiy, Y. M.; Zavracky, P. M.; McGruer, N. E.; Karger, B. L. *Anal. Chem.* **1997**, *69*, 426−430.
(41) Gatlin, C. L.; Kleemann, G. R.; Hays, L. G.; Link, A. J.; Yates, J. R., III. *Anal. Biochem.* **1998**, *263*, 93−101.
(42) Xu, N.; Lin, Y.; Hofstadler, S. A.; Matson, D.; Call, C. J.; Smith, R. D. *Anal. Chem.* **1998**, *70*, 3553−3556.
(43) Figeys, D.; Aebersold, R. *Anal. Chem.* **1998**, *70*, 3721−3727.
(44) Figeys, D.; Gygi, S. P.; McKinnon, G.; Aebersold, R. *Anal. Chem.* **1998**, *70*, 3728−3734.
(45) Lazar, I. M.; Ramsey, R. S., Sundberg, S.; Ramsey J. M. *Anal. Chem.* **1999**, *71*, 3627−3631.
(46) McCormack, A. L.; Schieltz, D. M.; Goode, B.; Yang, S.; Barnes, G.; Drubin, D.; Yates, J. R., III. *Anal. Chem.* **1997**, *69*, 767−776.
(47) Erdjument-Bromage, H.; Lui, M.; Lacomis, L.; Grewal, A.; Annan, R. S.; McNulty, D. E.; Carr, S. A.; Tempst, P. *J. Chromatogr. A* **1998**, *826*, 167−181.
(48) Posewitz, M. C.; Tempst, P. *Anal. Chem.* **1999**, *71*, 2883−2892.
(49) Lingner, J.; Hughes, T. R.; Shevchenko, A.; Mann, M.; Lundblad, V.; Cech, T. R. *Science* **1997**, *276*, 561−567.
(50) Zachariae, W.; Shevchenko, A.; Andrews, P. D.; Ciosk, R.; Galova, M.; Stark, M. J. R.; Mann, M.; Nasmyth, K. *Science* **1998**, *279*, 1216−1219.
(51) Yaron, A.; Hatzubai, Y. A.; Davis, M.; Amit, S.; Manning, A. M.; Andersen, J. S.; Mann, M.; Mercurio, F.; Ben-Neriah, Y. *Nature* **1998**, *396*, 590−594.
(52) Betts, J. C.; Blackstock, W. P.; Ward, M. A.; Anderton, B. H. *J. Biol. Chem.* **1997**, *272*, 12922−12927.
(53) Webb, Y.; Zhou, X.; Ngo, L.; Cornish, V.; Stahl, J.; Erdjument-Bromage, H.; Tempst, P.; Rifkind, R. A.; Marks, P. A.; Breslow, R.; Richon, V. M. *J. Biol. Chem.* **1999**, *274*, 14280−14287.
(54) Straight, A. F.; Shou, W.; Dowd, G. J.; Turck, C. W.; Deshaies, R. J.; Johnson, A. D.; Moazed, D. *Cell* **1999**, *97*, 245−256.
(55) Dole, M.; Mach, L. L.; Hines, R. L.; Mobley, R. C.; Ferguson, L. P.; Alice, M. B. *J. Chem. Phys.* **1968**, *49*, 2240−2249.
(56) Thomson, B. A.; Iribarne, J. V. *J. Chem. Phys.* **1979**, *71*, 4451−4463.
(57) Yamashita, M.; Fenn, J. *J. Chem. Phys.* **1984**, *88*, 4451−59.
(58) Aleksandrov, M. L.; Gall, L. N.; Krasnow, N. V.; Nikolayev, V. I.; Pavlenko, V. A.; Shkurov, V. A. *Dokl. Phys. Chem.* **1985**, *277*, 572−76.
(59) Meng, C. K.; Mann, M.; Fenn, J. B. *Z. Phys. D* **1988**, *10*, 361−368.
(60) Fenn, J. B.; Mann, M.; Meng, C. K.; Wong, S. F.; Whitehouse, C. M. *Science* **1989**, *246*, 64−71.
(61) Schmelzeisen-Redeker, G.; Bütfering, L.; Röllgen, F. W. *Int. J. Mass Spectrom. Ion Processes* **1989**, *90*, 139−150.

Briefly, electrospray commences when an applied voltage reaches a threshold value. At this potential, the electrostatic force (p_E) pulling a solution toward the interface plate balances the force (p_γ) associated with the surface tension acting to retain the liquid in the capillary. Under the influence of the electric field, the liquid at the tip of the sprayer becomes dielectrically polarized. As the applied voltage exceeds this threshold, the electrostatic force causes the polarized liquid at the tip of the capillary to undergo a conformational change to a liquid cone. At the pointed end of the cone, p_γ can no longer withstand the attraction of the electric field, causing small, electrically charged droplets to detach. The size of these highly charged droplets has previously been determined to be proportional to the flow rate. As such, lower flows are more desirable, as they generate droplets with much higher combined surface-to-volume ratios, allowing larger portions of the analyte molecules to become available for desorption. Since electric fields are orthogonal to conductors, these small droplets, upon detachment from the liquid cone, immediately accelerate toward the interface plate. Their movement is slowed by collisions with surrounding air molecules and, in some instruments, nitrogen curtain gas. During this flight, considerable evaporation occurs at the surface of the droplets. As they become smaller, charge density increases, leading to a series of fission steps, which generate ever smaller progeny droplets until, ultimately, the release of a single detectable ion. It is is believed that each fission step results in a 15% loss of detectable ions, further substantiating the value of initial small droplet formation.

We find that exact manufacture and quality control of spray needles with specific orifice diameters, in combination with precisely controlled helium backpressure and applied voltage, will generate stable nanoflows, down to 1−2 nL/min. At those ultralow flows, the sensitivity is substantially increased, the result of improved "overall ion transfer efficiency" (tip-to-detector). Positioning and applied potential of the spray needle are exceedingly important, however, to obtain quality MS/MS spectra at analyte concentrations of ≤5 fmol/μL.

EXPERIMENTAL SECTION

Chemicals. β-galactosidase (*Escherichia coli*) and ammonium bicarbonate were purchased from Sigma (St. Louis, MO); acetonitrile was from Burdick & Jackson (Muskegon, MI); formic acid from Fluka (Ronkonkoma, NY); and trypsin was "modified sequencing grade" from Promega (Madison, WI). Peptide mixtures were generated by resuspending β-galactosidase to 5 μg/μL in 100 mM ammonium bicarbonate and digesting with trypsin (E/S: 1/20; w/w) for 3 h at 37 °C. After incubation, the resulting mixture is diluted with 30% acetonitrile/0.1% formic acid to a 1 pmol/μL stock and frozen in 35-μL aliquots. Final concentration of the control is adjusted by further diluting the freshly thawed stock solution (in 30% acetonitrile/0.1% formic acid) just before use. Yeast glucose-6-phosphate dehydrogenase (G6PD) tryptic peptide mixture was a gift from Hediye Erdjument-Bromage and had been prepared exactly as described.[47]

Table 1. Molecular Ions Used for Analysis

ion	*m*/*z*	charge state	sequence
1	533.8	2+	WVGYGQDSR
2	593.0	3+	IENGLLLLNGKPLLIR
3	671.2	2+	VDEDQPFPAVPK
4	871.8	2+	LSGQTIEVTSEYLFR

Mass Spectrometry. All experiments were performed with a modified API 300 triple-quadrupole mass spectrometer (PE Sciex, Thornhill, Canada). The micro-ion spray source was replaced with the JaFIS. The API 300 instrument does not allow for user control of the curtain plate voltage, so a Y-connection was inserted between the ring and the curtain plate to set them to the same potential. The source interlock assembly was removed to allow greater accessibility to the front end of the vacuum chamber, and a jumper was installed in the source interlock circuitry to simulate an ion spray source. No nebulizing gas or sheath flow was employed. Ultrahigh purity nitrogen was used as a curtain gas at a flow rate of 0.55 to 0.81 L/min. Ionization source (IS) potential ranged from 350 to 3500 V depending on the flow rate. The voltages for the orifice and the ring were set at 5 and 350, respectively, for flow rates ≥4 nL/min; the ring potential was reduced to 200 V for flow rates <4 nL/min.

The instrument was calibrated and its performance verified by using the JaFIS to infuse a polypropylene glycol (PPG) standard solution, provided by the manufacturer, diluted 1:10 in 33% acetonitrile/0.1% formic acid. For calibration of the mass filters, the resolutions of the Q1 and Q3 quadrupoles were set to unit resolution (0.7 ± 0.1 amu full-width/half-maximum (fwhm)) for the mass to charge 59, 175, 616, 907, 1255, 1545, 2010, and 2242 ions from the solution. Since the intent of our source design was to achieve maximum sensitivity for MS/MS analysis of proteolytic peptides, the resolution of the first quadrupole was reduced to transmit the complete isotopic envelope of the precursor ion. Except where otherwise noted, all single MS scans were collected using a 0.2 amu step size and a 5 ms dwell time over a mass range from 400 to 1400 amu; all product ion scans were collected using a 1 amu step size and a 5 ms dwell time over a mass range from 100 amu to the singly charged mass of the precursor ion with a 50 mmu/amu mass defect utilizing the peak hopping functionality of the LC2Tune software. For statistical analysis, 12 scans were averaged (5 min), and four ions were arbitrarily selected from the β-galactosidase peptide mixture for use in determining background-subtracted signal intensities; those ions and the corresponding tryptic peptide sequences are listed in Table 1.

Matrix-assisted laser-desorption/ionization (MALDI) time-of-flight (TOF) mass spectrometry was done using a REFLEX III (Brüker-Franzen, Bremen, Germany) instrument equipped with a gridless pulsed-extraction ion source and a 2-GHz digitizer and was operated in reflectron mode, as described.[47] Spectra were obtained by averaging signals from multiple laser shots.

(62) Smith, R. D.; Loo, J. A.; Edmonds, C. G.; Baringa, C. J.; Udseth, H. R. *Anal. Chem.* **1990**, *62*, 882−899.
(63) Sakairi, M.; Yergey, A. L.; Siu, K. W. M.; LeBlanc, J. C. Y.; Guevremont, R.; Berman, S. S. *Anal. Chem.* **1991**, *63*, 1488−1490.
(64) Fenn, J. B. *J. Am. Soc. Mass Spectrom.* **1993**, *4*, 524−535.
(65) Tang, L.; Kebarle, P. **1993**, *65*, 3654−3668.
(66) Winger, B. E.; Light-Wahl, K. J.; Ogorzalek Loo, R. R.; Udseth, H. R.; Smith, R. D. *J. Am. Soc. Mass Spectrom.* **1993**, *4*, 536−545.
(67) Wang, G.; Cole, R. B. *Anal. Chem.* **1995**, *67*, 2892−2900.
(68) Fernandez de la Mora, F.; Loscertales, I. G. *J. Fluid Mech.* **1992**, *243*, 561−574.
(69) Kabarle, P.; Tang, L. *Anal. Chem.* **1993**, *65*, 972A−986A.
(70) Juraschek, R.; Dülcks, T.; Karas, M. *J. Am. Soc. Mass Spectrom.* **1999**, *10*, 300−308.

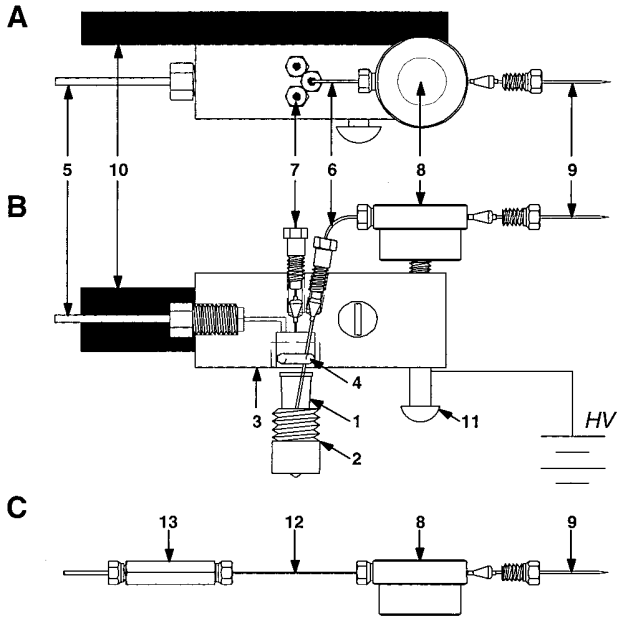

Figure 1. Schematic diagram of an in*J*ection *a*daptable *F*ine *I*onization *S*ource ("JaFIS") with PCR-tube (A, top view; B, side view) or capillary (C) type sample reservoirs: 1, sample reservoir (PCR tube); 2, nylon collar; 3, sample holder; 4, O-ring; 5, pressure/vent line; 6, pickup line; 7, through ports; 8, ion spray body; 9, ion spray needle (ISN); 10, Delrin shaft; 11, voltage connector; 12, sample capillary; 13, union. More details are to be found in the Experimental and Results sections.

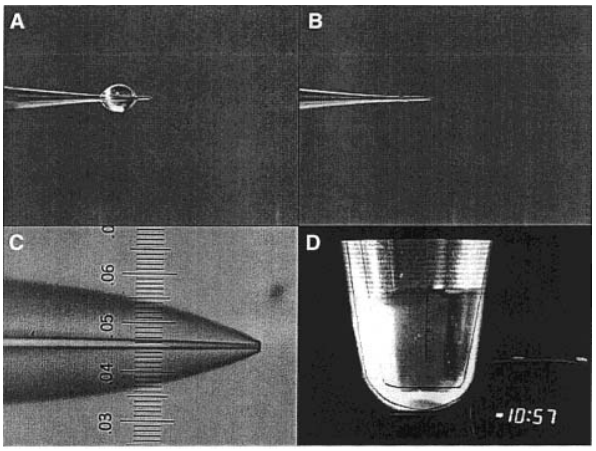

Figure 2. Interactive aspects of JaFIS operation and quality control. Pressurized ion spray needle, positioned ~6 cm from the curtain plate and containing liquid sample, with ion spray potential toggled between 0 V (panel A) and 1500 V (panel B); microscopic view (Nikon Optiphot-2, with 100× objective) of pointed end of ion spray needle (panel C); (smallest division on the "ruler" equals 0.8 μm); magnified view of a PCR-type sample reservoir on a video monitor (panel D) (liquid levels tracked using a calibrated acetate sheet attached to the 13-in. screen (±0.2 μL accuracy) and flow rate calculated from changes over time).

Construction of Ionization Source. The JaFIS assembly used in this study was derived from an earlier described version;[36] a schematic view of the newer type is given in Figure 1A,B. A 0.2-mL PCR tube (United Scientific Products, San Leandro, CA), with the cap removed, was selected as the sample reservoir (#1) because it provided us with the smallest volume and a high degree of manufacturing uniformity (as necessitated by PCR applications). The reservoir is inserted into a nylon collar (#2), which is then threaded into the socket of a Teflon sample holder (#3), containing a Viton O-ring (#4) (Part No. 9464K13; MacMaster Carr, New Brunswick, NJ) as a pressure seal. A pressure/vent line (#5) made of $^1/_{16}$-in. o.d./800-μm i.d. Teflon is attached to the rear of the sample holder using a $^1/_4$ in.-28 Teflon ferrule and bushing (PE Applied Biosystems, Foster City, CA) and connects to a pressure regulation station constructed in-house (see below). A 365-μm o.d./25-μm i.d., 55-mm long piece of fused silica capillary (FSC) tubing (Polymicro Technologies, Phoenix, AZ) functions as a pickup line (#6) and is inserted through the sample holder into the reservoir and sealed into place using a polyimide 0.4-mm i.d. ferrule (Part No. FS.4-5; Valco Instrument Corp., Houston, TX) with a long, $^1/_{32}$-in. stainless steel bushing (Valco Part No. LZN.5). The internal dead volume of the pickup line is ≤28 nL. A second and third through port (#7) are available in the top of the sample holder for (i) installation of either a platinum electrode and/or a transfer line from an autosampler and (ii) a vent line connected to an electronically actuated low dead volume valve. The ability to depressurize the sample reservoir allows for easy changing of the ISN with minimal sample loss. The outlet of the pickup line is connected to the ion spray body (ISB; #8) through another 0.4-mm i.d. ferrule with a standard, $^1/_{32}$-in. stainless steel bushing (Valco Part No. ZN.5). The ISB consists of a 0.15-mm bore/0.5-mm long stainless steel microvolume connector (Valco Part No. MU.5XTI).

The ion spray needle (ISN or sprayer; #9; Figure 2A−C) is a 30-mm long piece of FSC (75, 50 or 25-μm i.d./ 365-μm o.d.) which has been narrowed at one end using a P-2000 laser-based micropipet puller (Sutter Instruments, Novato, CA). First, the fused silica is cut to 6-in.-long pieces and 1 cm of the protective coating removed at the center using a MicroSolv CE polyamide stripping tool (Scientific Resources, Inc). Once pulled apart, the two equal halves are inspected/calibrated using an Optiphot-2 microscope (Nikon Inc., Melville, NY) with a dry 100× objective and measuring reticule (Figure 2C) and then stored in tightly sealed plastic boxes. Great care must be taken when handling the sprayers; they are very fragile and, when left out for extended periods of time, can accumulate moisture and dust from the air. Prior to installation, the distal end of the ISN is cut to exact length and connected to the ISB in the same way as the pickup line. The internal dead volume of the connector, which serves as the electrical/analyte liquid interface, is ~10 nL. The ISB is attached to the sample holder, and the sample holder to a 0.5-in. diameter Delrin shaft (#10) using round head screws (10−32 × 1 $^1/_4$ in.). The ion source potential is supplied to the ISB from the ion source voltage connection on the API 300 through the vertical screw (#11).

Alternatively, the sample can be sprayed out of a microcapillary (#12 in Figure 1C; 365-μm o.d./variable i.d.). Capillaries of ≥75 μm i.d. are filled by simple capillary action at ambient pressure; narrower capillaries require a pressurized filling-station. The connection to the ISB is exactly as described above for the pickup line. The other end is connected to a $^1/_{16}$-in., low dead volume internal union (#13; Valco Part No. ZU1C) using a $^1/_{16}$-in./0.4-mm polyimide ferrule (Valco Part No. FS1.5) and standard $^1/_{16}$-in. stainless steel bushing. The opposite end of the union is connected to a pressure source (not shown) using $^1/_{16}$-in. o.d./

0.8-mm i.d. Teflon tubing (Part No. 20106; Alltech Associates, Deerfield, IL). A standard, $^1/_{16}$-in. stainless steel bushing and ferrule (Valco Part Nos. ZN1 and ZF1) ensure a pressure tight connection.

The pressure control system consists of a 0−60 psi regulator (Porter Instrument, Hatfield, PA) with a 0−30 psi gauge (McMaster-Carr) and a purge valve (Whitey, Highland Heights, OH) connected to the gauge port of the reducer. The regulator is connected to an ultrahigh purity helium source and the pressure/vent line via double end shut-off quick-connects (Swagelock Quick-Connect Co., Hudson, OH). The entire pressure control system is mounted in an aluminum utility case (Newark Electronics, Chicago, IL) for ease of handling.

The JaFIS is positioned through the use of three stepper-motor driven translation stages, with 2-μm resolution and a translation speed of 2 cm/s (Newport Corp., Irvine, CA.), assembled in an $x-y-z$ configuration. The stages are controlled by a motion controller/driver model MM3000 (Newport) and a Macintosh Powerbook G3 (Apple Computers, Cupertino, CA) interfaced with a PCMCIA GPIB card (National Instruments, Austin, TX). Positioning of the ISN relative to the orifice is accomplished through a pair of high-resolution, magnifying CCD cameras with 9-in. monitors (Chugai Boyeki, Japan). A third CCD camera and 13-in. monitor (Panasonic/ Matsushita, Japan) permits tracking of liquid level in the sample reservoir or observation of the ionization process at the sprayer tip (Figure 2D). Lighting is provided by fiber optic illuminators (Dolan-Jenner Industries, Woburn, MA). The translation stages, cameras, and the mass spectrometer are mounted to a vibration-proof table (Newport). Instrument control software (ICS) was developed on the Powerbook G3 using LabView (National Instruments) to permit movement of the source by discrete increments in all three axes as well as saving optimized locations. The ICS has three preset positions: "Change ISN", "View", "Extend", and a user-defined position, "Spray", for rapid and reproducible positioning of the source. Briefly, "Change ISN" positions the source for easy accessibility for sample and ISN replacement; "View" positions the tip of the ISN directly in front of the third CCD camera, ∼6 cm from the curtain plate, for flow inspection or scanning the length of the ISN for air bubbles or particulates; "Extend" translates the source to a safe distance (6 mm) right in front of the orifice where the ISN is within the viewing field of the positioning cameras but no corona discharge will occur, not even at an ISP of 1500 V; and "Spray" is defined by the user as the optimal position for maximum signal strength.

Operation of the Source. Utilizing the ICS, the source is translated to the "Change ISN" position, where the sample reservoir is threaded into the sample holder and/or, if so required, a new ISN installed. The source is then moved to the "View" position, where the integrity of the electrical−liquid interface is inspected, and the pressure is slowly increased until migration of the meniscus can be viewed throughout the flow path. The ISN is monitored until the flow path is completely purged of all interspersed gas pockets, which have been found to impede sprayer performance. Since JaFIS is typically operated at flow rates between 2 and 80 nL/min, and with a tip-to-tube volume of ∼160 nL, the time required to prime the source may vary between 2 and 80 min. Once all air is displaced, a small droplet forms at the tip of the ISN (Figure 2A), and ion source (IS) voltage should be toggled between 0 and 1500 V (or 3500 V at higher flows) to confirm electrical continuity throughout the flow path. If the droplet dissipates when voltage is applied and a new one appears when voltage is removed, as illustrated in Figure 2 (panels A−B), the integrity of the electrical−liquid interface has been established. Once this is done, the source is translated to the "Extend" position, approximately 3−4 mm in front of the instrument orifice. During translation to the "Extend" position, the ion source potential is reduced to 1000 V, as excessive field strength has been found to cause cavitation and/or cracking of the sprayer, leading to unstable if not complete loss of signal. Once extended, the position and IS are optimized empirically (from the initial positioning as close as possible to the predetermined ideal location; see Results) by monitoring nonaveraged MS spectra. Once optimized, the "Spray" position of the source is saved and experimental data acquisition can be initiated.

The typical time for ISN installation and optimizing of the spray is 25 min, of which 10 min is used to adjust the position and ion source potential (ISP). At 4 nL/min, this process consumes ∼40 nL, or only 2% of a typical 2-μL sample volume, an important practical advantage of the JaFIS technology. Since the longevity of noncoated (i.e. nonmetallic) sprayers has been demonstrated to be on the order of days,[36] the optimization procedure is required only once, at startup, provided that the flow path is not permitted to run dry. This is frequently done using a standard peptide solution, thereby further limiting consumption of precious analyte. Manual sample exchanges can be completed in less than 2 min; however, the time frame for analysis of an exchanged sample is entirely dependent upon the tip-to-tube volume and flow rate.

Measuring Optimum ISN Position and Flow. Before positional effects of the ISN on signal intensity (i.e. ion transmission) can be studied, a frame of reference must be agreed upon to define the theoretical (and calibrate experimental) three-dimensional coordinates. As shown in Figure 3, the long (z) axis of the mass spectrometer (parallel to the quadrupole rods) is theoretically situated dead center of the circular orifice (where, by definition, the x and y axes intersect) and through the cross-hairs of all three quadrupoles, hence, defining the ideal ion path. The experimentally calibrated "Zero $x-y-z$" ($x,y,z = 0,0,0$) position was then located in the following way. With the aid of magnifying cameras pointing from different angles, the tip of the ISN was positioned inside the orifice (250-μm diameter; PE-SCIEX specifications), then slowly moved to the left until it touched the side, and then carefully up or down until judged to be level with the orifice center. This precise location was experimentally defined as $x = -125$, $y = 0$ (in μm). The plane of the orifice was located along the z-axis ("$z = 0$") by placing a small piece of Parafilm (measured to be 100-μm thick) in front of it and moving the ISN slowly forward until it touched (as judged from a subtle rippling); this spot was defined as $z = -100$ (in μm), completing calibration.

Flow rates were determined by tracking the liquid level in the sample reservoir. While in the "Spray" position the sample tube is directly in front of the third CCD camera. A calibrated overlay attached to the 13-in. monitor provides indication of actual sample volume (±200 nL accuracy; Figure 2D), and flow rate is calculated from changes in volume over time (typically overnight). Flow rates

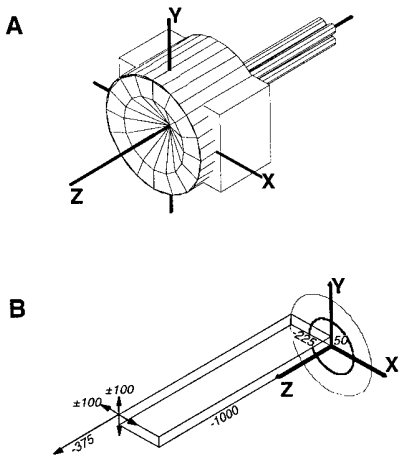

Figure 3. Definition of *x,y,z*-axes and positioning of the ion spray needle. Panel A illustrates the spatial arrangement of all three axes relative to the position of the quadrupole rods; *x* and *y* are situated in the plane of the orifice and intersect with *z* dead center. The drawing as shown is based on the API300 system from PE-SCIEX. Panel B shows the optimal position of the spray needle tip (flow rate, 4 nL/min; potential, 600 V) at *x,y,z* coordinates of −225,50,−1000 (in μm; with tolerances of ±100,±100,−375); for details, see the results section.

were recalibrated each time the ISN or pressure had been changed.

An extended series of reiterative optimization experiments indicated a practical, highest-efficiency ISN position for any given flow rate/ISP combination. The systematic analysis data are discussed under Results.

RESULTS AND DISCUSSION

Ion Spray Needle Development. The JaFIS was designed as a variable-flow nanoelectrospray device capable of operating reproducibly, and with the same ease of use, over a wide range of user-defined flow rates. To that end, a number of ISN aperture i.d./pressure combinations were examined to determine the optimal flow rates associated with each; our investigation was limited to flow rates lower than 200 nL/min, specifically to those less than 20 nL/min. Despite recent advances in the coating technology to extend longevity of a metallic layer,[32,71−73] coated ISNs offer no practical advantages over uncoated, JaFIS-configured ones;[36] hence, coated needles were not studied here.

Fused silica capillaries of varying i.d. were taken for pulling ISNs while keeping the o.d. constant at 365 μm for reasons of rigidity and simplicity in connecting to the ISB. After lengthy experimentation with the micropipet puller, we empirically devised a series of four-line programs that reliably provided ISNs with aperture i.d. ranging from 0.8 to 5.6 μm, at precise 0.8-μm increments, from capillaries with an initial i.d. of 75 μm. We then investigated the effects of the helium pressures and the ISPs to determine the most stable and reproducible flow rates for each aperture. Table 2 summarizes the results of these experiments, indicating that a stable spray at flows as low as 1−2 nL/min (≤625 V ISP) can be achieved. Additional combinations of aperture i.d. and pressure were evaluated, but those listed in Table 2 gave the most stable and reproducible results over extended time periods. Since not all applications require low flows, the data in Table 2 may guide the user to select the most desirable conditions for any given application. For instance, the low-flow (≤4 nL/min) capability of JaFIS enables adequate analysis of exceedingly small sample volumes by still providing lengthy analysis times (hours); faster flows allow for higher-throughput scenarios on larger volume samples. Indeed, with the ISN dead volume fixed at ∼130 nL, the selection of a flow rate must balance the higher sensitivity against the delay time associated with sample changeovers.

All of the data presented here were acquired using 75-μm-i.d. FSC sprayers. However, the use of smaller i.d. FSC is currently being explored to reduce the overall sprayer dead volume. Preliminary data for 0.4- and 0.8-μm aperture sprayers pulled from 25-μm-i.d. FSC suggests that the resistance to flow from these smaller i.d. capillaries is significantly higher (Table 2; top line). Alternatively, shortening the length of the pickup line and ISN could be explored to minimize both dead volume and flow resistance with narrower capillaries.

As illustrated in Table 2, each specific aperture i.d./pressure combination results in a certain window of flow rates. This is due to small particles accumulating in the capillary near the tip, effectively reducing aperture i.d. Observation of ISNs using the magnifying CCDs revealed these particles being carried to the tip by the air−liquid interface and liquid flow through the sprayer, particularly at high initial flow rates. It was found that the accumulation of these particles could be greatly reduced by slowly (as opposed to instantly) ramping the pressure to the target setting during purging. Increasing the pressure to maintain a given flow rate as the effective inner diameter becomes reduced was found to only worsen the accumulation process; instead the position and ion spray potential are reoptimized until the flow rate stabilizes. Examination under the microscope revealed these particles to be fragments of fused silica and dust remaining in the capillary from manufacturing and cutting. Almost all reduction in flow rate seems to occur in the first hour, after which the flow rate stabilizes and remains constant during further ISN usage. In those instances in which the flow path has been completely obstructed the sample reservoir is vented, voltage removed, and the ISN replaced with minimal loss of sample or no loss at all if the needles are pretested, which can be easily done off-line. No reduction in flow rate or additional accumulation has been observed in association with serial analysis of multiple samples using the same ISN. This can be attributed to the fact that all samples had been passed over a microtip of Poros 50 R2[47] beads for concentration/extraction, which also act as a mechanical sieve to trap contaminating particles.

Optimization of ISN Position and Ion Spray Potential. In the electrospray process, a "Taylor cone"[31] forms when the applied voltage reaches a threshold voltage. At this potential, the electrostatic force (p_E) pulling the solvent toward the interface plate balances the force (p_γ) associated with the surface tension acting to retain the liquid in the capillary. As the applied voltage exceeds this threshold, the electrostatic force dominates and droplets are drawn from the Taylor cone as the electrospray process commences:

(71) Kriger, M. S.; Cook, K. D.; Ramsey, R. S. *Anal. Chem.* **1995**, *67*, 385−389.
(72) Valaskovic, G. A.; McLafferty, F. W. *Rapid Commun. Mass Spectrom.* **1996**, *10*, 825−828.
(73) Kelly, J. F.; Ramaley, L.; Thibault, P. *Anal. Chem.* **1997**, *69*, 51−60.

Table 2. Flow Rates and Operating Conditions for Given Ion Spray Needle Inner Diameters and Applied Backpressures[a]

tip orifice i.d. (μm)	psi	flow rate (nL/min)	ISP (V)	Δ(ISP) (V)	*z*-axis (μm)	Δ *x*-axis (μm)	Δ *y*-axis (μm)
~0.4	17	0.8−2	360−440	80	−500 (−150)	±75	±75
0.8	10	1−6	550−700	150	−1000 (−375)	±100	±100
1.6	10	10−20	700−950	250	−1500 (−650)	±150	±150
1.6	15	20−30	1000−1350	350	−1750 (−750)	±150	±150
2.4	6	20−40	1000−1500	500	−2000 (−1000)	±250	±220
2.4	8	40−70	1400−2000	600	−2500 (−1500)	±425	±400
5.6	2	70−150	1800−2550	750	−3000 (−1500)	±1100	±875
5.6	4	150−250	2500−4000	1500	−4000 (−2000)	±1100	±875
10.0	2	200−400	2750−4500	1750	−5000 (−2000)	±1100	±875
10.0	4	300−500	3500−6000	2500	−5000 (−2000)	±1100	±875

[a] Flow rates vary with manufacturing-dependent variance of tip-ID and with pressure (psi value for each tip is the median, giving a flow rate about halfway in the range listed). ISP is given as the window of optimum voltage (Δ, width in V) to be used with the corresponding flow rates. *x*, *y*, and *z* axes are as defined in Figure 3. The positons along the *z*-axis are listed for every tip-ID/psi combination; only negative values (away from the orifice) are possible, and tolerances (listed in parentheses) only apply to being further away (−) from the orifice, as positioning closer will likely cause arcing at the corresponding voltages. Optimal positions along *x* and *y* axes were found to be 225 and 50 μm, respectively; the tolerances (Δ) are given in the respective columns. Definitions: i.d., inner diameter; psi, pounds per square inch; ISP, ion spray potential.

$$p_E = p_\gamma$$

However, in the JaFIS source design the introduction of an applied pressure (p_A) as the driving force for liquid flow should allow electrospray to occur at a lower electrostatic pressure:

$$p_E + p_A = p_\gamma$$

This reduces the threshold voltage and thus allows JaFIS to operate at lower applied voltages. Since the precise distance between the sprayer tip and the interface plate that is required to establish an electrospray varies with the square of the threshold voltage,[31] the reduction in voltage should in principle allow the JaFIS to operate within closer range of the orifice. The positioning of the tip in all three dimensions, relative to the orifice, was thereby found to be critical (see below); at these very low flows (≤2 nL/min) and close proximities, repositioning of less than 200 μm in or across the axis of the ion path, or a change in ISP of less than 100 V, had a deleterious effect on sensitivity.

To define the windows of movement in all three axes, as well as the associated ISP, for optimum signal strength for each of the flow rates listed in Table 2, the sprayer tip was positioned empirically and the ISP adjusted until the maximum signal strength was obtained. Once positioned, the values for each of the three axes, and the ISP, were recorded and 5 min of averaged MS data was acquired. Ion spray potential was then reduced in 50 V increments and 5 min of averaged single MS data acquired, again until the signal was lost; stable signal was restored at the previously noted optimum voltage and the process repeated by raising the ion spray potential until the signal was again lost. The ISP was then kept at its optimum value and the source translated in 500-μm increments in the axis of the ion path (*z*), and data reacquired until a stable signal could no longer be maintained (Figure 4; left panel). The source was subsequently returned to the optimum *z*-position and the process repeated, moving the source in 50-μm increments perpendicular to the axis of the ion path (*x* and *y*). For the purposes of routine operation, a "permissible window" was defined as the positional and voltage ranges that provided 80% or more of the optimum signal strength (Table 2).

As illustrated in Figure 4, the ideal position for acquisition of spectra at a flow of 4 nL/min is ~1 mm from the orifice, 225 μm to the left or right, and 50 μm above the center of the orifice (as pictured in Figure 3B). The permissible window was found to be −375 μm in the axis of the ion path and ±100 μm in each direction perpendicular to the ion path (Figure 3B; Table 2). By contrast, at 25 nL/min the optimum spray position was 1750 (−750) μm from the orifice, 225 ± 150 μm to the left/right, and 100 ± 150 μm above the center (data not shown). All this clearly demonstrates that it is now quite possible to move the ISN closer to the orifice at lower flow rates. It is essential, in fact, to do so if one is to take full advantage of the enhanced ion transfer and sensitivity (see section on ion transfer below). Higher flow rates are more tolerant of changes in position and ion spray potential (Table 2), but as clearly illustrated in Figure 5, the sensitivity is then greatly compromised. To obtain comparable signal strength at 25 nL/min, relative to 2.5 nL/min, it was necessary to increase the sample concentration 5-fold (from 50 to 250 fmol of tryptic peptide mixture/μL).

Figure 5 clearly shows that the optimum ion source voltage at a lower flow (2.5 nL/min) is ~600 V, which is similar to that used in conventional nanoelectrospray (580−800 V).[31,32] However, in conventional nanoelectrospray the interface plate is typically held at 100 V, whereas in our experiments the ring was set at 350 V. This equates to a potential difference of 250 V for JaFIS, at least 230 V less than what has been reported with earlier devices. In the same figure, the permissible windows (≥80% signal strength of maximum) for ion spray potential are compared for flows of 2.5 and 25 nL/min and found to be 595 ± 25 and 1200 ± 175 V, respectively. Thus, the window for optimal signal strength with respect to potential decreases markedly with a reduction in flow. At the lowest flow rates, a change in ion spray potential of 20 V can easily result in a 2-fold reduction of signal strength.

Effects of Field Strength. The interdependence of voltage and coaxial distance in maximizing ion signal is still better illustrated in Figure 6. In these experiments, the tip of the ISN was again incrementally positioned away from the interface plate in 1-mm steps, starting at 1 mm. At each spot, the ion source

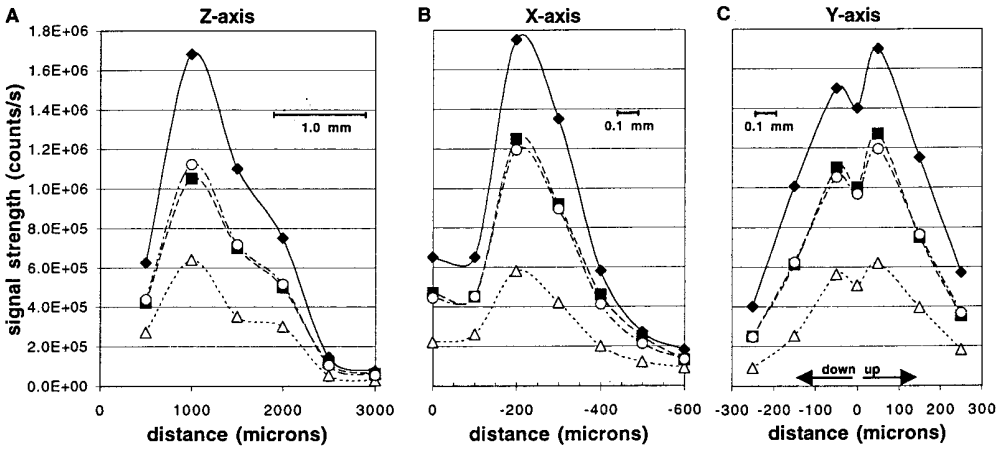

Figure 4. Effect of ion spray needle (ISN) positioning on signal strength. The sample (100 fmol of β-galactosidase tryptic peptides/μL of 0.1% formic acid in 30% acetonitrile/70% water) was sprayed at 4 nL/min, and at an ISP of 625 V, for single MS analysis using a PE-SCIEX API300 instrument fitted with a JaFIS. The spray position of the ISN was $x,y,z = -225,50,-1000$ (in μm); these distances were changed, one dimension at a time, as indicated on the panels. Signal strength (i.e. peak height) was determined for each of three selected ions (◆, 1; ■, 3; △, 4; key in Table 1) after baseline subtraction and using spectra obtained by summing 12 scans. The average signal for the three ions is also shown (○). More details are to be found in the Experimental and Results sections.

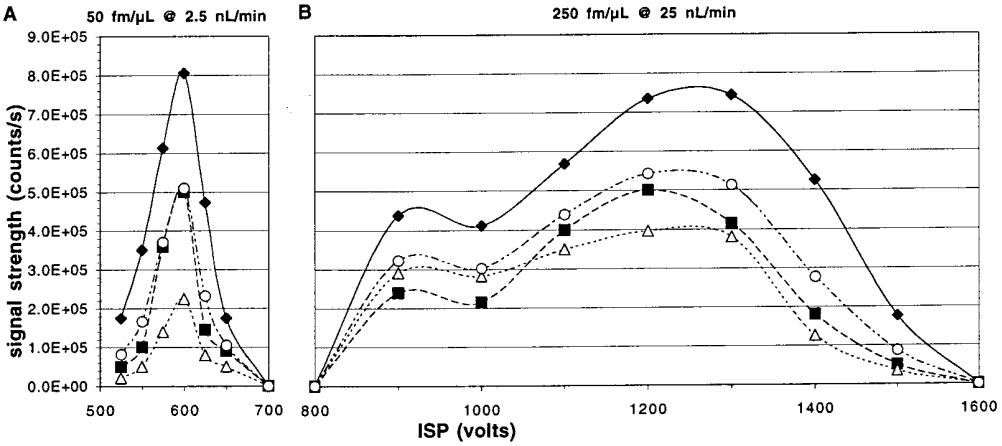

Figure 5. Effect of ion spray potential (ISP) on signal strength. Samples (see Figure 4), at concentrations of 50 and 250 fmol/μL, were sprayed at 2.5 nL/min (panel A) and 25 nL/min (panel B), respectively. ISN positions (x,y,z) were consistently held at $-225,50,-1000$ μm $-225,100,-1750$ μm, respectively; ISP was changed between 525 and 700 V and between 800 and 1600 V, respectively. Signal strength was determined for each of three selected ions (◆, 2; ■, 3; △, 4; key in Table 1) after baseline subtraction and using spectra obtained by summing 12 scans. The average signal for the three ions is also shown (○). More details are to be found in the Experimental and Results sections and under Figure 4. Note that ISP windows are nonoverlapping and that average signal strength is similar for both setups despite a 5-fold difference in analyte concentration.

voltage was either (A) kept constant at 600 V (optimum at 4-nL/min flow and 1-mm distance) or (B) reoptimized empirically and the corresponding maximum signals recorded. In the latter case, we observed that the optimum ISP increased by about 250 ± 100 V/mm, which also happened to be the difference between the ring and the preferred ISP at 1-mm distance (see above). For simplicity, the ISP was then raised stepwise by exactly 250 V/mm for the final measurements shown in panel B. At constant ISP of 600 V, the signal obtained from a 100-fmol/μL peptide solution fell sharply over just a short distance, to 47% at 2 mm and 6% at 3 mm (relative to 100% at 1 mm) and no measurable signal at 4 mm and beyond. By contrast, with holding of the electric field strength constant at 250 V/mm, the signal remained at about 25% of the "1-mm" value upon pulling back the needle to 3 mm and beyond; however, the initial drop that resulted from repositioning the ISN to just 2 mm off the orifice remained substantial (to ~60%). Similar results were observed at higher flow rates as well (data not shown). The data demonstrate that although ionization can be sustained at relatively greater distances through proper adjustment of the ISP (i.e. by restoring the field strength), there are deleterious effects on signal strength, i.e., on sensitivity.

The results from these experiments support the observations of other researchers who have found that electrospray performance is rather tolerant of changes in position and ion spray potential at the higher flow rates, potentials, and distances at which "standard" electrospray is typically done. However, sensitivity suffers by at least 1 order of magnitude. To operate at the short distances and low potentials necessary for utmost sensitivity, one must spray at exceedingly low flow rates (see below).

In optimization of the source position at these low flows, the ability to precisely position the ISN is paramount to success. The control and digital feedback provided by stepper-motor transla-

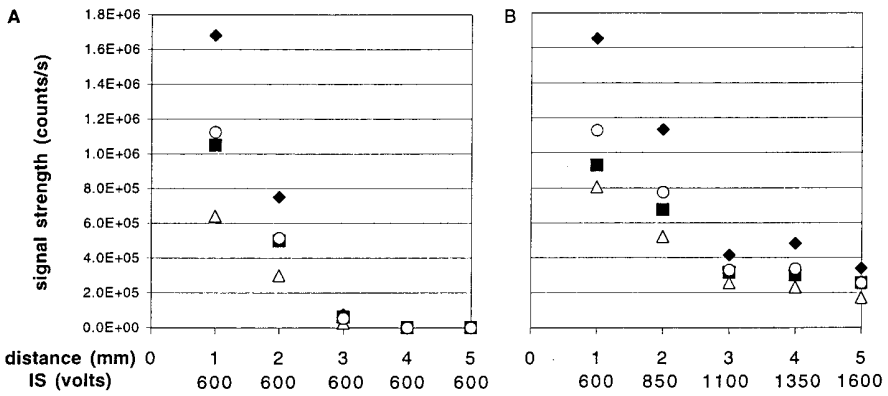

Figure 6. Effect of electrical field strength on signal. The sample (100 fmol/μL; see Figure 4) was sprayed at 4 nL/min. The spray position of the ISN was $x,y,z = -225,50,-1000$ (in μm). The distance along the z-axis was stepped to -5 mm (in 1-mm increments) between experiments, as indicated on the panels. ISP was either held constant at 600 V (panel A) or raised by 250 V/mm (panel B). Signal strength was determined for each of three selected ions (◆, 2; ■, 3; △, 4; key in Table 1) after baseline subtraction and using spectra obtained by summing 12 scans. The average signal for the three ions is also shown (○). More details are to be found in the Experimental and Results sections, and under Figure 4.

tional stages and motion controller are critically important. At flow rates ≤ 10 nL/min, the use of manual micromanipulators would be very difficult at best, but with the 2-μm resolution and 2 cm/s translation speeds of the motion controlling system used here, optimization is both simple and reproducible.

Flow Rate. Operation of previously described micro- and nanoelectrospray devices indicated that lower flow rates were more suitable for higher sensitivity due to better ion transfer and extended analysis times.[23,27,32,33] However, no systematic, quantitative efforts to analyze the effects of flow rate on ion transmission have been reported to date. Since we can generate any given flow (by selecting the previously determined optimum sprayer i.d./pressure combination; Table 2), and knowing the precise three-dimensional ISN position plus corresponding ISP for each, we carried out a series of experiments to examine signal strenghts over a wide range of flows. To this end, 2 μL of 100 fmol/μL β-galactosidase tryptic peptides was loaded into the sample reservoir and the JaFIS operated at 500, 400, 250, 150, 75, 50, 22.5, 4, 1.6, and 1.0 nL/min, each at settings for maximum signal strength. Twelve scans were averaged per experiment, and the baseline-subtracted signal of selected peaks were determined. The results shown in Figure 7A prove that, in the 75 → 1.6-nL/min range, lower flow translates to higher absolute signal strength. At 4 nL/min, the nominal flow rate of the JaFIS, the signal strength was four times higher than for conventional nanoelectrospray (~40 nL/min) and with at least a 6-fold increase in analysis time. Similarly, signal strengths are more than three times higher than at flow rates associated with commercially available micro-ionspray devices (100−200 nL/min) and with a 40-fold increase in analysis time. The importance of extended analysis times will be illustrated later on, analyzing proteolytic digests at 1 fmol/μL concentrations (Figure 9).

One important, practical aspect of the continuous nanoflow is a sometime gradual decrease, the result of particle buildup, as discussed. Instead of increasing the pressure when this happens, it is more helpful to reduce the applied voltage and move the ISN closer to the orifice until a stable ion current is restored. This has often resulted in better signal, turning potential disaster into advantage.

Ionization and Transfer Efficiencies. It is counterintuitive to assume that lower flow would translate to increased signal strength since the number of analyte molecules available for ionization/detection is volume dependent at a given concentration. For instance, a 100 fmol/μL solution sprayed at 22.5 nL/min would have ~1.35×10^9 molecules/min available whereas at 4 nL/min the same solution would have only ~2.41×10^8, yet the flow rate experiments above clearly demonstrated that lower flows produce higher signal strengths. In examinations of earlier nanoelectrospray devices, this increase in signal strength was directly related to greater ion transfer efficiencies at lower flows,[31,32] and we assumed this to be the case for the JaFIS as well.

To determine the ion transfer efficiencies at various flows, the signal strength data from Figure 7A were then used to calculate the ratio of the recorded number of analyte ions to the theoretical number of analyte molecules sprayed per unit time, in the manner previously described by Wilm and Mann.[32] These ratios, defined as "overall efficiencies", are presented in Figure 7B. Wilm and Mann have reported an overall efficiency of 1 in 390 on 200 fmol/μL of a synthetic peptide at a flow of 22 nL/min using their nanoelectrospray source on a Sciex API III instrument.[32] Using the JaFIS, our calculated efficiencies were 1 in 480 at 22.5 nL/min, remarkably close to the previously reported value, thereby lending credence to both old and new findings. For the nominal flow rate of the JaFIS (4 nL/min) then, an average overall efficiency of 1 in 50 was observed, an 8-fold improvement over conventional nanoflow. The maximum overall efficiency that we could achieve for a "100 fmol/μL" sample was 1 in 26, at a 1.6-nL/min flow.

Why does lower flow rate result in greater ion count, i.e., absolute signal strength? It has been shown that the radius of the zone of droplet emission from the Taylor cone (r_e) is proportional to the $^2/_3$-power of flow rate, $(dV/dT)^{2/3}$, and Wilm and Mann have calculated an r_e of 88 nm for a flow rate of 25 nL/min.[31] Using this relationship, the radius of emission from the JaFIS is estimated to be 26 nm at 4 nL/min, or approximately one-third of that at 25 nL/min. Smaller emission radii generate smaller droplets, which have a greater surface-to-volume ratio for more efficient desolvation. Since the tip of the ISN is only 1 mm

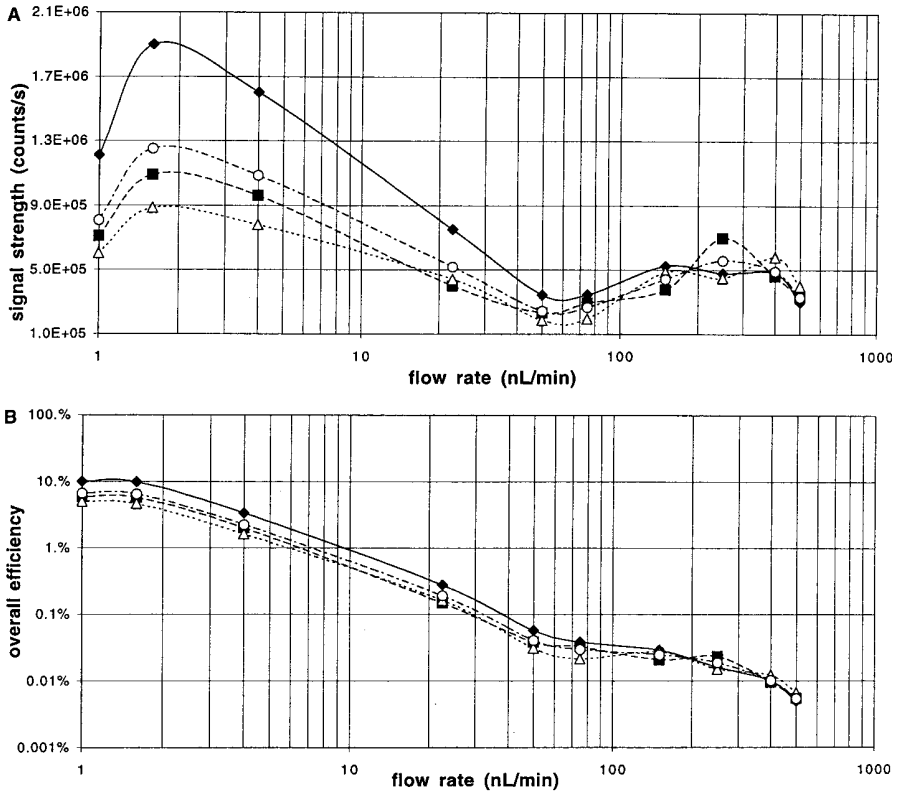

Figure 7. Effect of flow rate on signal strength and overall ion transfer efficiency. The sample (100 fmol/μL; see Figure 4) was sprayed at 1.0 nL/min (ISP = 400 V; $z = -0.5$ mm) or at 1.6 nL (560 V; −0.8 mm), 4 nL (625 V; −1 mm), 10 nL (800 V; −1.5 mm), 22.5 nL (1200 V; −1.75 mm), 50 nL (1600 V; −2.5 mm), 75 nL (2000 V; −3 mm), 150 nL (3000 V; −3.5 mm), 250 nL (3750 V; −4 mm), 400 nL (4000 V; −5 mm), and 500 nL (4500 V; −5 mm) per minute; *x* and *y* positions were always held at −225 and 50 μm, respectively. Panel A: signal strength was determined for each of three selected ions (◆, 2; ■, 3; △, 4; key in Table 1) after baseline subtraction and using spectra obtained by summing 12 scans. The average signal for the three ions is also shown (○). Panel B: overall ion transfer efficiency (tip-to-detector) is the percent ratio of the number of counts (i.e. ion events) versus total number of peptide molecules sprayed out of the capillary per equal time unit. Since the concentration remained unchanged, the number of peptide molecules presented for analysis is flow dependent. More details are to be found in the Experimental and Results sections, and under Figure 4.

away from the interface plate, inside the curtain gas region, these smaller diameter droplets are even more efficiently desolvated. In addition, the shorter distance limits expansion of the ion plume prior to reaching the orifice, thereby minimizing ion dilution in the gas phase and ensuring higher ion density in the transfer region immediately in front of the orifice. Because electric fields are orthogonal to conductors, the desolvated gas phase ions are then ejected directly into the vacuum region of the mass spectrometer.

One might speculate that there is a lowest flow rate at which all available analyte ions will enter the mass spectrometer. At this flow, the overall efficiency would equal 100%, and any further reduction would result in a loss of signal strength because fewer molecules are emitted from the sprayer per unit of time. The lowest reproducible flow rate that we can generate thus far is 1.0 nL/min. At this flow, the overall efficiency for a "100 fmol/μL" sample is calculated to be 1 in 26; the same, in fact, as at 1.6 μL/min. If the losses associated with the quadrupoles and ion optics are taken into account, this could very well be the flow rate at which all available ions are transmitted. We have experimented with sub-nL/min flows but have observed severe baseline anomalies at lower mass (data not shown), which may be associated with clustering. Techniques normally used to alleviate clustering, such as filling the collision cell with gas and/or increasing the transmission energy through the second quadrupole, tend to result in lower sensitivity and as such are not desirable in our case.

Analyte Concentration. Having determined the dependence of signal strength upon positional, potential, and flow rate changes, we wanted to explore the relationship between signal strength and analyte concentration using the JaFIS. Tryptic digest mixtures of β-galactosidase were prepared at concentrations of 5, 10, 25, 50, 100, 250, and 500 fm/μL, and 3 μL of each was loaded consecutively into the JaFIS for analysis at a flow rate of 4 nL/min. Figure 8 illustrates the baseline-subtracted signal strengths observed in these experiments; JaFIS signal appears linear at 4 nL/min at concentrations between 10 and 50 fmol/μL and again from 50 to approximately 200 fmol/μL. However, the general trend is for signal strength to increase with concentration in a less than linear fashion. In fact, at concentrations above 200 fm/μL the relationship between concentration and signal strength appears to approach an asymptotic limit. It is assumed that this is due to the Rayleigh stability limit, which dictates the maximum charge density possible on a droplet of a given radius. The net charge on a droplet is a function of the number of ions present in the droplet, and the radius of a droplet emitted from the Taylor cone is proportional to the $^2/_3$-power of the flow rate; this limits the number of charged analyte molecules that can be transmitted per unit time. The limit has been expressed by Wilm and Mann[31] as

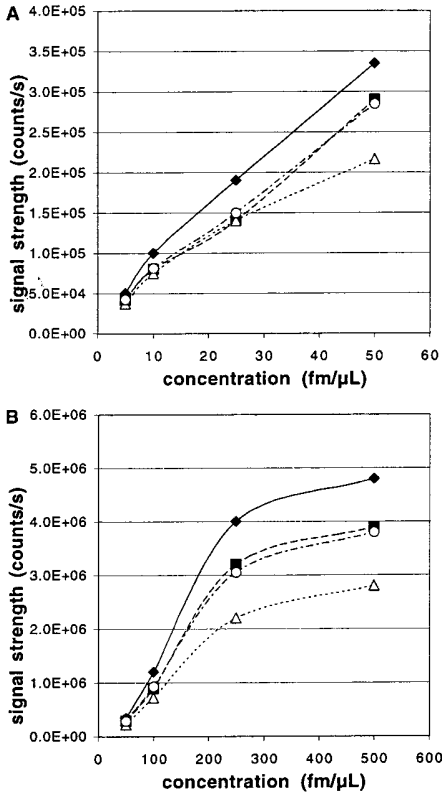

Figure 8. Effect of analyte concentration on signal strength. The sample (see Figure 4) was sprayed at 4 nL/min. The position of the ISN was *x,y,z* = −225,50,−1000 (in micron), and ISP was held at 625 V. Analyte concentration was as indicated, and the results are shown for 5−50 fmol/μL in panel A and 50−500 fmol/μL in panel B. Signal strength was determined for each of three selected ions (◆, 2; ■, 3; △, 4; key in Table 1) after baseline subtraction and using spectra obtained by summing 12 scans. The average signal for the three ions is also shown (○). More details are to be found in the Experimental and Results sections, and under Figure 4.

a maximum current, which can be calculated from the solvent surface tension γ and density ρ, the cone angle of the Taylor cone ϑ, and the ratio of applied voltage to threshold voltage necessary to generate the Taylor cone, U_a/U_T:

$$I_{max} = 12\pi\gamma\left(\frac{\epsilon_0 \tan\left(\frac{\pi}{2} - \vartheta\right)}{\rho}\right)^{1/2}\left\{\left(\frac{U_a}{U_T}\right)^2 - 1\right\}^{1/2}$$

The current observed on a mass spectrometer would be far less than this, however, reduced by the overall efficiency η of the electrospray process:

$$I_{obs} = \eta I_{max}$$

If one assumes a U_a/U_T ratio of 1.09 (the ratio used by Wilm and Mann; we have not yet determined U_T for the JaFIS), the maximum current can be calculated to be 3.59×10^{-9} amps with $\gamma = 0.0202$ N m^{-1}, $\rho = 930$ kg m^{-3} (30% acetonitrile[74]), and $\vartheta = 49.3°$. When the overall efficiency of JaFIS at 4 nL/min ($^1/_{50}$, or 2%) is applied, the observed current is expected to be 7.18×10^{-11} amps. This current may also be expressed in terms of the number of charges per ion and number of ions striking the detector (counts per second):

$$I_{obs} = \left(\frac{\text{charge}}{\text{ion}}\right)\left(\frac{\text{counts[ions]}}{\text{second}}\right)$$

If one assumes an average of two charges per β-galactosidase tryptic fragment, the actual observed current is calculated as 1.22×10^{-12} A, over 1 order of magnitude less than predicted. This discrepancy is most likely due to the fact that the solvent ions are also contributing to the observed current, which would in fact be equivalent to the total ion current (TIC):

$$I_{obs} = I_{analyte} + I_{solvent} \approx \text{TIC}$$

The experiment at 500 fmol/μL was repeated, monitoring the TIC while scanning over a mass range from 30 to 2000 amu to include as many solvent ions as possible, and a TIC of 3.65×10^8 counts/s was observed. From this total ion current the observed current was calculated as 5.84×10^{-11} A, assuming that the preponderance of singly charged solvent ions shifts the average charge per ion to one. This observed current based on the total ion current is in excellent agreement with that predicted above.

The Rayleigh stability limit's determination of the maximum signal strength due to *all* ions and the overall efficiency's dependence upon flow rate implies that there is a maximum observable TIC for any given flow, regardless of analyte concentration.[31] This has been verified empirically using the JaFIS; of all experiments and analyses performed, no total ion currents have been observed over 1×10^9 counts/s, and TICs in the range of 10^8 counts/s have been observed only at the lowest flows. It is our belief that the increases in signal strength are not linear with increases in concentration due to this dependence of the ion current on contributions from both analyte and solvent ions. In order for the analyte ion current to increase, the solvent ion current must decrease by an equivalent amount. As the number of analyte ions increase with concentration, they must displace twice as many solvent ions due to the difference in charge, and this becomes more difficult as the concentration approaches that limited by the Rayleigh stability criterion.

Sequence Analysis of Peptide Mixtures. From the results in Figure 8, it is evident that usable signal can be obtained by ESI(JaFIS)-MS analysis from peptide solutions at a concentration of 5 fmol/μL without any prior trace enrichment (i.e. by capillary liquid chromatography). As only 12 scans had been averaged, the appreciable signal-to-noise derived solely from the excellent ion transfer at low nL/min flows. We therefore wanted to explore the lower limits of MS/MS-based sequence analysis of peptide mixtures when averaging really large numbers of scans. The time factor associated with such an approach is a valid option with typical sample volumes of 1−4 μL and flow rates of ≤ 4 nL/min. We selected G6PD tryptic peptides for this study because this mixture had previously been carefully calibrated and mass analyzed.[47] Although the system is to be considered "artificial", we carried out a series of MS analyses that resembled a regular protein identification project. Thus, a 0.5-μL aliquot of a 1 fmol/

(74) Lide, D. R., Ed. *CRC Handbook of Chemistry and Physics*, 71st ed.; CRC Press: Boca Raton, FL, 1990−1991.

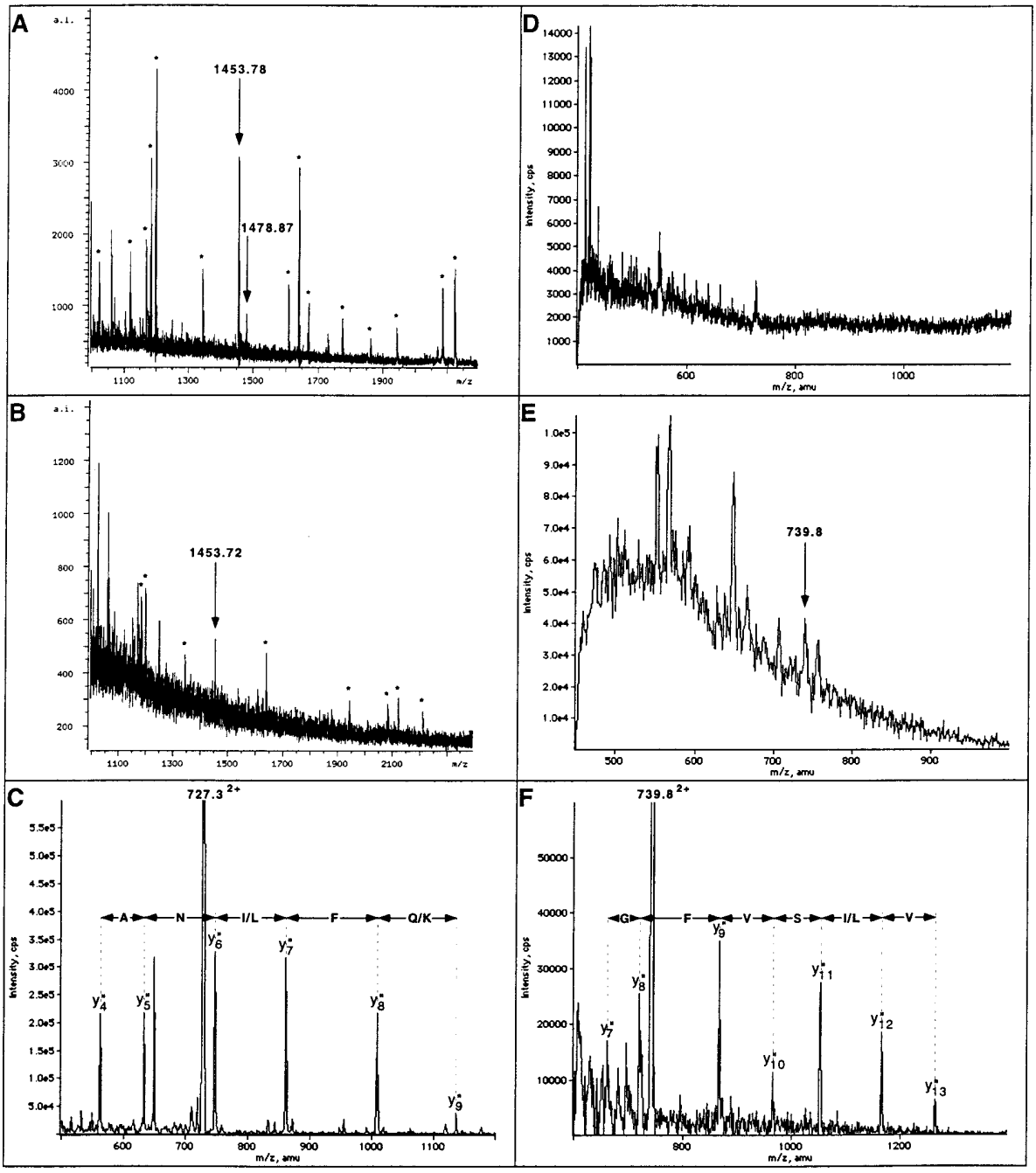

Figure 9. Multimode mass spectrometric analysis of peptide mixtures. G6PD tryptic peptides (1 fmol/μL 0.1% formic acid in 30% acetonitrile/70% water) were analyzed by MALDI-reTOF MS (0.5 μL sample applied; 150 scans summed, panel B) or continuous flow ESI(JaFIS) MS or MS/MS (1.6 nL/min; 560V; $x,y,z = -225,50,-800$ μm; scans of 1-amu step size and 6-ms dwell time over a 400−1400 amu mass range, panels C−F). Panel A shows a MALDI-reTOF spectrum of a 10-fold-concentrated sample (0.5 μL). In panels A and B, peaks of *m/z* corresponding to the theoretical, monoisotopic $[M + H]^+$ of predicted tryptic G6PD peptides are indicated with either an asterisk or with the actual numerical value; panel D, Q1 scan (600 scans averaged); panel E, precursor ion scan using the Val immonium ion (mass 72) as the indicative fragment (600 scans averaged); panels C and F, MS/MS spectra (1000 scans averaged each) acquired for ions at *m/z* 727 (marked as 727.3^{2+}) and 740 (739.8^{2+}), respectively. Limited y″ ion series were assigned together with the amino acid sequences derived from it. Peaks marked with 1453.78 and 1453.72 in panels A and B are the singly charged molecular ions corresponding to the doubly charged precursor ion in panel C; peak 1478.87 in panel A is the singly charged ion corresponding to the doubly charged precursor ions in panels E and F. More details are to be found in the Experimental and Results sections.

μL solution was first analyzed by MALDI-TOF MS. A number of peaks that were clearly over background corresponded to m/z values matching the calculated monoisotopic mass of predicted G6PD tryptic peptides in protonated form (Figure 9, panel B). A rather lengthy (~1 h) Q1 scan of the same sample did not yield usable data (panel D).

In a first scheme, MALDI-TOF results were then taken to calculate m/z values of the hypothetical doubly and triply charged

ions, which were used to delimit ion transmission through Q1 in subsequent tandem MS experiments. As many as 1000 scans were averaged over a total analysis time of nearly 2 h per predicted precursor ion. The result of one such experiment is shown in panel C. MS/MS of the doubly charged ion (m/z = 727.3) that corresponds to the peak marked with an arrow in panel B (m/z = 1453.7) yielded an easy-to-read sequence, sufficient to make an identifcation in the nrNCBI database using the SequenceTag algorithm.[20] In case of an unknown protein, MS/MS of the hypothetical triply charged ion (m/z = 485.2) would also have been done, adding an additional 2 h to the analysis time.

In a complementary approach, a lengthy precursor ion scan (panel E; 600 scans averaged) was done in search of peptides that had gone undetected in the MALDI-TOF analysis. The precursor ion marked with an arrow had no singly charged counterpart in the MALDI-TOF spectrum (panel B) and was therefore selected for MS/MS analysis (panel F). A usable sequence was obtained in this case as well. Just to independently confirm the presence of this peptide in the digest mixture, a 5 fmol aliquot (0.5 μL of a 10 fmol/μL solution) was also analyzed by MALDI-TOF (panel A) and the corresponding, small peak (m/z = 1478.8) is marked with an arrow. The latter experiment was for the purpose of developing the methods and for clarity of the presentation only; it was not essential for obtaining the results shown in the other panels.

The electrospray part of the entire procedure (both schemes; assuming that two MS/MS experiments had to be done on the peptide selected from the MALDI-TOF data) outlined above took about 8 h to complete and consumed less than 1 μL, i.e., less than 1 fmol of peptide mixture. To this should be added 500 amol from MALDI-TOF analysis and about 500 amol (500 nL) for each additional peptide selected for sequencing. In all, then, 2−4 fmol of a peptide mixture in a 2−4 μL volume is sufficient, under fully optimized conditions, to confidently identify a protein. We realize, however, that a typical digest volume is about 1 order of magnitude larger. Thus, in a final experiment, we took 20 μL of a β-galactosidase tryptic digest in a 500-amol/μL concentration and containing 100 mM bicarbonate and 0.02% Zwittergent 3-16, typical additives to our *in-gel* digests (Lacomis, Erdjument-Bromage, and Tempst, unpublished procedure), loaded it on a 1.5-μL bed-volume RP-microtip, and eluted with 3 μL of 0.1% formic acid/30% acetonitrile.[47] From the recovery of a radiolabeled peptide, added to the mixture as a tracer, we calculated that about 60% had eluted from the tip, i.e., ~6 fmol of many, but not all, peptides. Following the exact same procedure as outlined above, partial sequence was derived from MS/MS data obtained from a triply charged cation of m/z = 593.0, as shown in Figure 10.

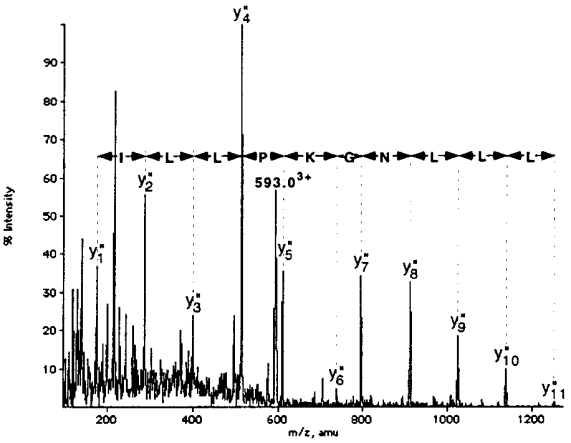

Figure 10. Microtip/nanoES(JaFIS) MS/MS of dilute peptide mixtures. A sample containing 10 fmol of β-galactosidase tryptic peptides in a 20-μL bicarbonate solution (plus 0.02% Zwittergent 3-16) was passed over a RP-microtip[47] and collected in a 3-μL final volume for MALDI TOF MS and for nanoES(JaFIS) precursor ion (mass 86) scan and MS/MS of selected ions. The MS/MS spectrum of the doubly charged ion at m/z 593 (593.0^{3+}) is shown, together with the y″ ion series and the amino acid sequence derived from it; Leu and Ile are denoted on the basis of the known β-galactosidase sequence, as they are indistinguishable by mass. Experimental conditions were as described under Figure 9 and in the Experimental and Result sections.

CONCLUSIONS

As an outgrowth of the various genome projects that have filled sequence repositories forthwith, structural chemists and biologists alike have eagerly embraced mass spectrometry as a novel and, by now, primary tool for protein identification. Like microchemistry before, much of this newer analytical facility resides in specialized resource laboratories. The success rate of such an operation depends not only on the available levels of sophistication and expertise to obtain quality data from minute amounts of (frequently contaminated) sample, but on doing so all the time. This second requirement is subject to the customary determining factors for routine analysis, namely ease-of-use and adequate throughput and fault tolerance. Perfection and high volume are not incompatible, nor should they be the exclusive province of ultraspecialized technology centers. Thus, we sought to assemble and optimize a continuous flow nanoelectrospray (nanoES[31,32]) source for high-performance analysis on a routine basis. Previously, we described an in*J*ection *a*daptable *F*ine *I*onization *S*ource ("JaFIS") that incorporated the desired practical features.[36] The current study was aimed at maximizing its performance, more specifically sensitivity. A systematic examination, and subsequent optimization, of several key experimental variables was therefore conducted.

We find that design, manufacture, and quality control of spray needles with specific orifice diameters, in combination with precisely controlled helium backpressure and applied voltage, will generate stable nanoflows, down to 1−2 nL/min, for hours to days on end. At those ultralow flows, positioning of the spray needle and the ion spray potential are exceedingly important. Repositioning by less than 0.5 mm or shifts in potential by as little as 25 V can cause a 2-fold drop in signal strength. The upside of low flows are prolonged analysis times and, remarkably, increased sensitivity for peptide analytes at concentrations of 100 fmol/μL and below, the result of greatly improved "overall ion transfer efficiency" (needle-to-detector). We have calculated these overall efficiencies to be 1/5600 (~0.02%), 1/480 (~0.2%), and 1/26 (~4%) at flows of respectively 250, 22, and 1.6 nL/min.

Used in combination with an off-line, microsample chromatographic device ("microtip"),[47,48] the optimized JaFIS implements simple "infusion-style" ESI-MS at levels of sensitivity approaching those of coupled capillary LC-MS. Although the concentration factor may be about 4- to 5-fold less with a microtip, the improved ion transfer efficiencies at ultralow flows should compensate. Indeed, we find a 3- to 4-fold increase in sensitivity when spraying at 1.6 nL/min as compared to 150−400 nL/min, flow rates typically

associated with cLC or CZE interfaces. Moreover, available spraying times in excess of 10−20 h allow for any number of tandem mass spectrometric analysis routines (e.g. different precursor ion scans; MS/MS on many peptides) to be performed and to average literally thousands of scans in each experiment, thereby improving signal-to-noise ratios, i.e., sensitivity. Translated into purely practical terms, we show that comprehensive analysis can be done on 2 fmol of a peptide mixture in a 2 μL volume, even when using a multimode MS approach. Such sample is readily prepared over an RP-microtip from a 10 fmol/20 μL proteolytic digest mixture, which, in turn, should be obtainable from 20−40 fmol of protein in a gel slice.

Furthermore, unlike in LC-MS type analyses, in our system all analyte ions are available at all time throughout the experiment. Conceivably, with the proper data dependent and analysis software, it might then be possible to confidently identify several proteins in a nonequimolar, heterogeneous mixture based on peptide mass fingerprinting (by MALDI-TOF and/or single quadrupole scan) followed by just a minimum number of carefully targeted MS/MS experiments, this on the basis of a reiterative process consisting of JaFIS-MS (and sometimes MS/MS) and then several rounds of data sorting, database searching, subtractive analysis, and MS/MS of selected peptides. Work is ongoing in our laboratory to further develop this concept.

ACKNOWLEDGMENT

The authors are indebted to Hediye Erdjument-Bromage and all colleagues from the Protein Center for providing materials and reagents and for advice, experimental help, and discussion; we thank Tom Covey and Matthias Wilm for sharing unpublished observations and discussion. This work was supported by Development Funds from NCI Grant P30 CA08748.

Received for review September 15, 1999. Accepted November 19, 1999.

AC991071N